

Various Models Mimicking the SM Higgs Boson ^a

Jung Chang¹, Kingman Cheung^{1,2}, Po-Yan Tseng¹, and Tzu-Chiang Yuan³

¹ *Department of Physics, National Tsing Hua University, Hsinchu 300, Taiwan*

² *Division of Quantum Phases and Devices, School of Physics,
Konkuk University, Seoul 143-701, Republic of Korea*

³ *Institute of Physics, Academia Sinica, Nangang, Taipei 11529, Taiwan*

(Dated: April 1, 2022)

Abstract

This review is based on the talk presented at the SUSY 2012 (Beijing). The new particle around 125 GeV observed at the Large Hadron Collider (LHC) is almost consistent with the standard model Higgs boson, except that the diphoton decay mode may be excessive. We summarize a number of possibilities. While at the LHC the dominant production mechanism for the Higgs boson of the standard model and some other extensions is via the gluon fusion process, the alternative vector-boson fusion is more sensitive to electroweak symmetry breaking. Using the well known dijet-tagging technique to single out the vector-boson fusion mechanism, we investigate potential of vector-boson fusion to discriminate a number of models suggested to give an enhanced inclusive diphoton production rate.

^a Invited review in *Int. J. Mod. Phys. A* **27**, 1230030 (2012), based on the plenary talk given at the 20th International Conference on Supersymmetry and Unification of Fundamental Interactions (SUSY 2012), Peking University, Beijing, China August 13, 2012 - August 18, 2012

I. INTRODUCTION

In this talk, we are going to summarize a few models that have been suggested to explain the newly observed particle of about 125 GeV at the Large Hadron Collider (LHC) [1, 2]. It is of very high expectation that the observed particle is the long-sought Higgs boson, which was proposed in 1960s [3].

Before the LHC era there have been many speculations of the breaking of electroweak symmetry (EWSB). There are two known scales in particle physics – the electroweak scale and the Planck scale. The fundamental Higgs boson of order 100 GeV is unstable against the radiative corrections. The so-called gauge hierarchy problem requires new physics has to come in around TeV scale in order that the unnatural cancellation between the bare mass term and the higher-order terms of the Higgs boson mass is under control. Historically, there are two categories of models: one with a strongly-coupled EWSB sector and one with a weakly-coupled EWSB sector. The most studied model for strong EWSB is the technicolor-type model [4] while that for weakly-coupled EWSB model is the supersymmetry [5]. In technicolor models, the standard model (SM) is simply an effective model below TeV scale, at which the theory is replaced by another strong dynamics. Therefore, the cutoff scale now becomes just TeV. On the other hand, supersymmetric models predict another set of particles, which differ from their SM counter parts by a half-integral spin. Quadratically divergent contributions to the Higgs boson radiative corrections are cancelled among the SM particles and the corresponding supersymmetric particles.

If the Superconducting Super Collider (SSC) were built the Higgs boson could have been discovered in early 2000s with perhaps a short running of the machine. Since the Higgs boson has been hiding for such a long time, many interesting alternatives were proposed in the last 10–15 years. Around the turn of the century extra dimension models became very popular, not to mention there have been a large number of varieties– large extra dimension [6], universal extra dimension [7], Randall-Sundrum models [8], etc. There are also the little Higgs type models [9]. In contrast to supersymmetry the new particles have the spin as their SM counter parts. Contributions to the Higgs boson radiative corrections are cancelled among the SM particles and the corresponding new particles. Perhaps, more and more models would have been proposed if the Higgs boson kept hiding. Wouldn't it be more fascinating for theorists?

The past few years the high energy community has been very excited with a number of experimental anomalies from the Tevatron, LHC, and dark matter (DM) experiments. The long-time inconsistency among the DAMA results [10] (also the CoGeNT [11]) and the other direct detection experiments has motivated a number of unconventional dark matter models [12, 13], such as inelastic DM [14], isospin-violating DM [15], multi-component DM [16], etc. The top-quark forward-backward asymmetry observed by the CDF and DØ collaborations is rather puzzling too [17]. Many models such as flavor-changing Z' , unusual W' , axigluon, etc [18] were proposed, but the new LHC results seem ruled out almost all of these models [19]. The CDF Wjj anomaly in 2011 [20] also stimulated a large number of theoretical or phenomenological models to account for the observation [21]. However, with non-observation of the resonance from DØ and CMS [22] the excitement gradually died out.

At the end of 2011, both the ATLAS and CMS [23] experiments at the LHC have seen some excess of events of a possible Higgs candidate in the decays of $h \rightarrow \gamma\gamma$, $h \rightarrow WW^* \rightarrow \ell\nu\ell\nu$ and $h \rightarrow ZZ^* \rightarrow 4\ell$ channels. Finally, the discovery was jointly announced in July 2012 by ATLAS [1] and CMS [2]. All the observed channels, WW , ZZ and $\gamma\gamma$ are consistent with the predictions of the SM Higgs boson, except that the $\gamma\gamma$ rate is somewhat higher than expectation. The $b\bar{b}$ and $\tau\tau$ channels are not confirmed yet, because of large uncertainties.

The diphoton production rate is about a factor of 1.3 – 2 higher than that of the standard model Higgs boson, while the ZZ^* and WW^* rates are consistent with the SM Higgs boson within uncertainties. Nevertheless, the observed rates are consistent with either the SM Higgs boson or some other Higgs models. A large number of models have been put forward to account for the observed particle at 125 GeV, including the SM, MSSM, NMSSM, UMSSM and other MSSM-extended models, fermiophobic Higgs, 2HDM, RS radion, inert-Higgs doublet, triplet Higgs models, etc.

The $H \rightarrow \gamma\gamma$ events collected by CMS and ATLAS can be divided into two categories: *inclusive* $\gamma\gamma X$ and *exclusive* $\gamma\gamma jj$ (though both experiments have more refined sub-divisions among various classes of events). Presumably, the inclusive $\gamma\gamma X$ events include all production channels such as gluon fusion, vector-boson fusion, associated production, etc, among which gluon fusion dominates for production of the SM Higgs boson and most of the models considered in this talk, except for the fermiophobic Higgs boson. On the other hand, exclusive $\gamma\gamma jj$ events mainly come from vector-boson fusion and associated production, which can be further disentangled by jet-tagging techniques. The vector-boson fusion produces ener-

getic forward jets while associated production with a W or Z produces jets with $m_{jj} \approx m_W$ to m_Z . The current evidence of the Higgs boson in the diphoton channel comes mainly from inclusive $\gamma\gamma X$ events, simply because the inclusive event rate is much higher than the exclusive $\gamma\gamma jj$ event rate.

The main goal of this talk is to summarize all the models and find the parameter space of each model that have been proposed to explain the excess in the inclusive Higgs diphoton events, and attempt in distinguishing the models using the exclusive $\gamma\gamma jj$ channel in vector-boson fusion (VBF) [24]. The exclusive VBF events with $\gamma\gamma jj$ in the final state are selected using the forward jet-tagging techniques which will be explained shortly. We will first choose the parameter-space region of each model that can account for the excess in the inclusive diphoton rate, and then in that region of parameter space we calculate the exclusive $jj\gamma\gamma$ VBF production rates. We found that the exclusive $\gamma\gamma jj$ production rate in VBF channel can give more information to help in distinguishing a number of popular models.

We summarize a number of models that have been used to account for the excess in the inclusive $\gamma\gamma X$ data as follows.

1. The SM Higgs boson [3] is still believed to be the most desirable candidate. It is still consistent with the data within uncertainty.
2. The lighter Higgs boson of the minimal supersymmetric standard model (MSSM) can acquire a large radiative correction from the top-stop sector to achieve a mass of 125 GeV, though it has been shown rather difficult to achieve an enhanced diphoton rate [25, 26]. However, it is possible when one of the staus is light enough, just above the LEP limit, and so the diphoton branching ratio is enhanced [25].
3. One of CP-even Higgs bosons in the next-to-minimal supersymmetric standard model (NMSSM) can account for the observed 125 GeV boson with an enhanced diphoton rate [27]. It could be the lightest or the second lightest one. The $U(1)$ -extended MSSM (UMSSM) [28] and other extensions [29] are also possible to account for the observed boson. The analyses for these extended MSSM models are much more involved and deserve dedicated studies.
4. The lighter CP-even Higgs boson of various types of the two-Higgs-doublet models (2HDM) [30], which has enough free parameters in the model that allows one to

achieve a large branching ratio into $\gamma\gamma$.

5. In the fermiophobic (FP) Higgs boson model, the Higgs boson is only responsible to generate the masses to W and Z bosons while the fermion masses are generated by some other means. Since the FP Higgs boson does not couple to the quarks, it cannot be produced via gluon fusion at hadronic colliders, but only through the VBF and the associated production with a vector-boson. Nevertheless, the FP Higgs boson lighter than 130 GeV has a much larger branching ratio into diphoton, such that it can still account for the observed inclusive diphoton rate at the LHC [31].
6. In Ref. [32], it was pointed out that the Randall-Sundrum (RS) radion, with enhanced couplings to gg and $\gamma\gamma$ due to trace anomaly, can explain the excess in the inclusive diphoton production rate and suppressed WW and ZZ rates, which provides the most economical alternative solution to explain the observed data.
7. The inert-Higgs-doublet model (IHDM) [33], which is a special case of 2HDM, in which one of the doublets entirely decouples from the leptons, quarks, and gauge bosons while the other one takes on the role of the SM Higgs doublet. The production rate of the Higgs boson is the same as the SM one. However, the decay width of $h \rightarrow \gamma\gamma$ can be enhanced by the presence of the charged Higgs boson in the loop. It was shown [33] that the diphoton production rate can be enhanced by a factor of about 1 – 2.
8. There may also be some possibilities that the SM-like Higgs boson first decays into two light scalar or pseudoscalar bosons, followed by subsequent decays into collimated pairs of photons, which appear as two photons in the final state [34]. On the other hand, instead of top-down approaches, it would also be useful to reversely determine the couplings and the nature of the observed 125 GeV particle by studying all the available data [35].

The disadvantage of gluon fusion is that it is not clear what particles and their masses running in the triangle loop. In some models, the contribution from a particular charged particle can increase or decrease the diphoton decay width, depending on the relative signs. For example, in the supersymmetric models, there are additional sfermions, charginos, charged Higgs bosons running in the loop, and therefore resulting in complicated dependence on the model parameters. On the other hand, the advantage of using WW fusion or associated

production with a W or a Z boson is that the production diagram is clean and directly testing the couplings of hWW and hZZ . Furthermore, the WW fusion has a cross section at least a factor of 2 larger than the associated production. We therefore focus on WW fusion. The WW fusion can be extracted by the presence of two energetic forward jets. We can impose selection cuts to select jets in forward rapidity and high energy region [36, 37]. By combining the production rates in the inclusive $\gamma\gamma X$ and exclusive $\gamma\gamma jj$ channels, one can obtain useful information about the nature of the 125 GeV new particle recently observed at the LHC.

We calculate the event rates in the WW fusion channel for a number of models that have been used to interpret the current LHC data of the 125 GeV ‘‘Higgs boson’’. The theoretical cleanliness of WW fusion has been explained in the last paragraph. We believe that the WW fusion channel can provide useful information to discriminate various models. The organization of this paper is as follows. We briefly highlight a number of models in the next section, and the WW fusion and selection cuts in Sec. III. We give the decay branching ratios in Sec. IV and production rates in Sec. V. We conclude in Sec. VI.

II. MODELS

A. Standard Model Higgs Boson

The SM Higgs boson [3] is still the most favorable candidate to interpret the observed boson, though the experimental data showed slightly excess in inclusive $\gamma\gamma X$ events over the prediction of the SM Higgs boson [1, 2]. Production of the SM Higgs boson is dominated by gluon fusion, which is an order of magnitude larger than the next important mechanism – VBF.

B. Two-Higgs-Doublet Model (2HDM)

There are two Higgs doublets instead of just one in the 2HDM. In order to avoid dangerous tree level flavor-changing neutral currents, the popular 2HDMs are imposed a discrete symmetry. In the type I, all of the fermions couple to a single Higgs doublet, and do not couple to the second doublet; while in the type II, one doublet couples only to down-type quarks and another doublet couples to the up-type quarks. In this talk, we focus on the

type II, which has the same Higgs sector as the MSSM. The Higgs sector consists of two Higgs doublets

$$H_u = \begin{pmatrix} H_u^+ \\ H_u^0 \end{pmatrix}, \quad H_d = \begin{pmatrix} H_d^+ \\ H_d^0 \end{pmatrix},$$

where the subscripts u, d denote the right-handed quark singlet field that the Higgs doublet couples to. The electroweak symmetry is broken when the Higgs doublet fields develop the following VEVs:

$$\langle H_u \rangle = \begin{pmatrix} 0 \\ v_u \end{pmatrix}, \quad \langle H_d \rangle = \begin{pmatrix} 0 \\ v_d \end{pmatrix}.$$

Physically, there are two CP-even, one CP-odd, and a pair of charged Higgs bosons after electroweak symmetry breaking (EWSB), and the W and Z bosons as well as the SM fermions, except for neutrinos, acquire masses. The Yukawa couplings and masses for fermions can be obtained from the following Yukawa interactions after EWSB

$$\mathcal{L}_{\text{Yuk}} = -y_u \overline{Q}_L u_R \tilde{H}_u - y_d \overline{Q}_L d_R H_d + \text{h.c.}$$

where $\tilde{H}_u = i\tau_2 H_u^*$. The parameters of the model in the CP-conserving case include

$$m_h, m_H, m_A, m_{H^\pm}, \tan \beta \equiv \frac{v_u}{v_d}, \alpha$$

where α is the mixing angle between the two CP-even Higgs bosons. There are enough free parameters in the Higgs potential such that all the above parameters are free inputs to the model, in contrast to the MSSM where the Higgs potential is highly restricted by supersymmetry in addition to gauge symmetry.

The couplings of the two lighter and heavier CP-even Higgs bosons h and H respectively and the CP-odd Higgs boson A to the top, bottom quarks, and taus are given by, with a common factor of $-igm_f/2m_W$ being suppressed,

	$t\bar{t}$	$b\bar{b}$	$\tau^-\tau^+$
h :	$\cos \alpha / \sin \beta$	$-\sin \alpha / \cos \beta$	$-\sin \alpha / \cos \beta$
H :	$\sin \alpha / \sin \beta$	$\cos \alpha / \cos \beta$	$\cos \alpha / \cos \beta$
A :	$-i \cot \beta \gamma_5$	$-i \tan \beta \gamma_5$	$-i \tan \beta \gamma_5$

while the charged Higgs H^- couples to t and \bar{b} via

$$\bar{b}tH^- : \frac{ig}{2\sqrt{2}m_W} [m_t \cot \beta (1 + \gamma_5) + m_b \tan \beta (1 - \gamma_5)].$$

Other relevant couplings in WW fusion are those to gauge bosons are given by,

$$\begin{aligned} hW^+W^- &: ig m_W \sin(\beta - \alpha) g^{\mu\nu} , \\ hZZ &: ig m_Z \frac{\sin(\beta - \alpha)}{\cos \theta_W} g^{\mu\nu} . \end{aligned}$$

Dominant production of the light CP-even Higgs boson h at the LHC is via gluon fusion, similar to the SM Higgs boson with the top quark running in the loop; however, in the large $\tan \beta$ region the bottom-quark contribution can also be substantial. Since the bottom-Yukawa coupling can be substantially enhanced, the gluon fusion cross section can be larger than the SM. On the other hand, since the couplings of the h to the WW and ZZ are simply the SM values multiplied by $\sin(\alpha - \beta)$, WW fusion cross sections are in general smaller than the SM.

The decay into two photons is somewhat more complicated than the SM. Besides the couplings hWW , $ht\bar{t}$, and $hb\bar{b}$ are different, there are also the charged Higgs bosons running in the loop. The charged Higgs boson couples to the light CP-even Higgs with the coupling [26]

$$\lambda_{hH^+H^-} = \frac{m_h^2 - \lambda_5 v^2}{m_W^2} \cos(\beta + \alpha) + \frac{2m_{H^\pm}^2 - m_h^2}{2m_W^2} \sin(2\beta) \sin(\beta - \alpha) . \quad (1)$$

However, the $b \rightarrow s\gamma$ and B meson mixing constraints require the charged Higgs boson mass $m_{H^\pm} > 500$ GeV for intermediate to large values of $\tan \beta$ [38]. We will choose $m_{H^\pm} = 500$ GeV in our analysis below.

The overall diphoton production rate $\sigma(gg \rightarrow h) \times B(h \rightarrow \gamma\gamma)$ in gluon fusion can easily vary between 0.5 – 2 of the SM prediction depending on parameters [30]. It was shown in Ref. [30] that the enhancement in branching ratio can be obtained roughly along $\sin \alpha$ near zero for all $\tan \beta$ in the type II model. We choose parameter space points there to illustrate.

C. Supersymmetric Higgs boson: MSSM

In order to achieve a mass of 125 GeV for the lighter CP-even Higgs boson, a very large radiative correction is needed, which essentially comes from top-stop loop. The approximate formula for the lighter CP-even Higgs boson is given by [25]

$$m_h^2 \approx m_Z^2 \cos^2 2\beta + \frac{3m_t^4}{4\pi^2 v^2} \left[\frac{1}{2} X_t + t + \frac{1}{16\pi^2} \left(\frac{3m_t^2}{2v^2} - 32\pi\alpha_s \right) t (X_t + t) \right] \quad (2)$$

where

$$X_t = \frac{2(A_t - \mu \cot \beta)^2}{M_{\text{SUSY}}^2} \left(1 - \frac{(A_t - \mu \cot \beta)^2}{12M_{\text{SUSY}}^2} \right), \quad t = \frac{M_{\text{SUSY}}^2}{m_t^2} \quad (3)$$

and $M_{\text{SUSY}} \sim 1$ TeV is the SUSY scale. A large A_t is needed to generate a large correction. Here we follow the findings in Ref. [25] for the parameter space: we choose $m_{Q_3} = m_{U_3} = 850$ GeV, $A_t = 1.4$ TeV, $m_A = 1$ TeV, and $\tan \beta = 60$. A detailed analysis of the MSSM parameter space based on Bayesian statistical analysis in light of the new observation of the 125 GeV Higgs candidate is also presented recently in Ref. [39]. The reason behind such a large $\tan \beta$ is the stau contribution to the diphoton branching ratio explained below [25].

In the production part via gluon fusion, the difference between the SM and supersymmetric models is that squarks also run in the triangle loop. As the experimental data have pushed the squark masses of the first two generations to be quite heavy but not the third generation (stop and sbottom) the change in production rates could be substantial, especially in large $\tan \beta$. On the other hand, the decay into diphoton is more involved in SUSY models. All charged particles, including squarks, sleptons, charginos, charged Higgs boson can flow in the triangle loop. With the present constraints from experiments, the production rate into diphoton (equal to production cross section times the branching ratio into diphoton) in the MSSM is shown to be very similar to the SM one and that the diphoton production rate can hardly be enhanced by more than a factor of 1.5 [25, 26, 39].

The formulas for the decay of the Higgs boson into two photons as well as production via gluon fusion can be found in Ref. [40]. The couplings of the lighter CP-even Higgs boson to the WW or ZZ are given by the SM ones multiplied by $\sin(\alpha - \beta)$. Therefore, the production rate in the WW fusion is in general similar to or smaller than the SM prediction.

We look at the parameter space in which the diphoton production rate would be larger than the SM value in the MSSM. It was shown in Ref. [25] that diphoton production rate can be larger than the SM one if one pushes the stau to be very light, just above the LEP limit. In addition to the above mentioned soft parameters, the other parameters are m_{L_3} , m_{E_3} , and the μ . Without loss of generality we choose [25]

$$m_{L_3} = m_{e_3} = 200 - 450 \text{ GeV} \quad \text{and} \quad \mu = 200 - 1000 \text{ GeV}, \quad (4)$$

in which we can scan for the diphoton production rate $\sigma(gg \rightarrow h)B(h \rightarrow \gamma\gamma)$ to be larger than the SM rate. The region essentially gives a light stau, which can enhance the $B(h \rightarrow$

$\gamma\gamma$). We will scan the region according to Eq. (4) and require the mass of the lighter CP-even Higgs boson around 125 GeV and the diphoton production rate larger than the SM value.¹

D. Fermiophobic Higgs

With the name “fermiophobic” (FP) the Higgs boson only couples to the vector bosons at tree level, though higher-loop corrections can induce small couplings to fermions. In this case, the Yukawa couplings and masses of fermions are generated by some other mechanisms, which are not of concern in this talk.

The coupling strength of the FP Higgs boson to vector bosons is the same as that of the SM Higgs boson. We write the interactions as

$$\mathcal{L}_{\text{FP}} = -gm_W h_{\text{FP}} W_\mu^+ W^{-\mu} - \frac{gm_Z}{2\cos\theta_W} h_{\text{FP}} Z_\mu Z^\mu. \quad (5)$$

Since the FP Higgs boson does not couple to quarks, it cannot be produced dominantly by gluon fusion at hadronic colliders, but only through the vector-boson fusion and the associated production with a W/Z boson. The corresponding production cross sections are the same as the VBF of the SM Higgs boson. Nevertheless, the FP Higgs boson lighter than 130 GeV has a much larger branching ratio into diphoton, such that it can still account for the observed diphoton rate at the LHC [31]. There are two reasons: (i) the FP Higgs boson decay into fermions is highly suppressed with only the loop-induced couplings, and (ii) the decay into photons is via a loop of W boson without the negative interference from the top quark. Thus, the branching ratio into diphoton can be enhanced by more than an order of magnitude. Overall, the diphoton production rate at the LHC is comparable to the SM Higgs boson, as was used to account for the observed boson [31]. An earlier study of FP Higgs boson at the LHC can be found in Ref. [42]. There is basically no free parameters in this model.

E. The Radion

The RS model [8] used a warped 5D space-time, a slice of the symmetric space AdS_5 , to explain the gauge hierarchy problem. The extra dimension φ is a single S^1/Z_2 orbifold with

¹ There is another possibility that the heavier CP-even Higgs boson can be at around 125 GeV and its diphoton production rates can be enhanced relative to the SM one [41]. We will not pursue this further here.

one hidden and one visible 3-brane localized at $\varphi = 0$ and π , respectively. It was pointed out by Goldberger and Wise [43] that the original RS model has a four-dimensional massless scalar (the modulus or radion) which does not have a potential and therefore the extra dimension cannot be stabilized. A stabilization mechanism was proposed in [43] by adding a bulk scalar field propagating in the background solution which can generate a potential to stabilize the modulus field. The minimum of the potential can be arranged to give the desired value of $kr_c \sim 12$ to solve the gauge hierarchy problem without extreme fine tuning of parameters. As a consequence, the lightest excitation mode of the modulus field is the radion, which has a mass of the order of 100 GeV to a TeV, and the strength of its coupling to the SM fields is of the order of $O(1/\text{TeV})$ [44]. Phenomenology of the stabilized radion and its effects on the background geometry were studied in [45].

The interactions of the stabilized modulus (radion) ϕ with the SM particles on the visible brane are completely determined by 4-dimensional general covariance. Thus the radion Lagrangian is given by

$$\mathcal{L}_{\text{radion}} = \frac{\phi}{\Lambda_\phi} T_\mu^\mu(\text{SM}) , \quad (6)$$

where $\Lambda_\phi = \langle \phi \rangle$ is of the order of TeV and T_μ^μ is the trace of the SM energy-momentum stress tensor, which has the following lowest order terms

$$T_\mu^\mu(\text{SM}) = -2m_W^2 W_\mu^+ W^{-\mu} - m_Z^2 Z_\mu Z^\mu + \sum_f m_f \bar{f} f + (2m_h^2 h^2 - \partial_\mu h \partial^\mu h) + \dots . \quad (7)$$

The coupling of the radion to a pair of gluons (photons) is induced at one loop level, with the dominated contributions coming from the heavy top quark (top quark and W) as well as from the trace anomaly in QCD (QED). The expressions of the induced couplings can be found in Ref.[32]. Similar to the SM Higgs boson, the dominant production channel for the radion is via gg fusion, followed by VBF [46]. In addition, $gg \rightarrow \phi$ gets substantial enhancement from the trace anomaly. For the decay of the radion, it is dominated by the gg mode instead of $b\bar{b}$ at the low mass region, while its diphoton branching ratio is merely a fraction of the SM value of $h_{\text{SM}} \rightarrow \gamma\gamma$.

Overall, the diphoton production rate $\sigma(gg \rightarrow \phi) \times B(\phi \rightarrow \gamma\gamma)$ can be larger than the SM rate if the scale Λ_ϕ is small enough, and as long as it is consistent with the search for RS graviton. If we do not concern about naturalness, the scale Λ_ϕ can be as small as 0.8 TeV. Here we fix the scale Λ_ϕ to be 0.8 – 0.99 TeV, which can enhance the diphoton production

rate in gluon fusion by a factor of $1.5 - 1.0$ [32] relative to the SM rate. Note that the branching ratios of the radion is independent of Λ_ϕ .

F. Inert Higgs Doublet Model (IHDM)

IHDM is a special case of 2HDM, in which one of the doublets takes on the role of the SM Higgs doublet, while the other one is inert which means that it entirely decouples from the SM leptons, quarks, and gauge bosons. The model also has an additional Z_2 symmetry, for which all SM particles are even, except for the particle content of the second inert Higgs doublet. The lightest Z_2 -odd particle of the second doublet can work as a candidate of dark matter. The Higgs sector consists of

$$H_1 = \begin{pmatrix} \phi_1^+ \\ \frac{v}{\sqrt{2}} + \frac{h+i\chi}{\sqrt{2}} \end{pmatrix}, \quad H_2 = \begin{pmatrix} \phi_2^+ \\ \frac{S+iA}{\sqrt{2}} \end{pmatrix}.$$

The electroweak symmetry is broken solely by one VEV:

$$\langle H_1 \rangle = \begin{pmatrix} 0 \\ \frac{v}{\sqrt{2}} \end{pmatrix}, \quad \langle H_2 \rangle = \begin{pmatrix} 0 \\ 0 \end{pmatrix}.$$

The Higgs potential is given by

$$V = \mu_1^2 |H_1|^2 + \mu_2^2 |H_2|^2 + \lambda_1 |H_1|^4 + \lambda_2 |H_2|^4 + \lambda_3 |H_1|^2 |H_2|^2 + \lambda_4 |H_1^\dagger H_2|^2 + \frac{\lambda_5}{2} [(H_1^\dagger H_2)^2 + \text{h.c.}]$$

Physically, there are 2 CP-even scalars (h, S), 1 CP-odd scalar (A), and a pair of charged Higgs (H^\pm). The h plays the role of the SM Higgs boson while the others are inert. A list of parameters of the model includes $m_h, m_S, m_A, m_{H^\pm}, \mu_2$, and λ_2 .

Production via gluon fusion and via WW fusion are the same as the SM Higgs boson. However, the decay into $\gamma\gamma$ receives additional contributions from the H^\pm running in the loop. If kinematically allowed the Higgs boson h can also decay into H^+H^- , AA , and SS . For simplicity and to achieve a large enough branching ratio into $\gamma\gamma$ we set the masses of S, A, H^+ to be above the threshold ($m_h/2$). In this model, the coupling between the charged Higgs boson and the SM Higgs boson h is given by

$$g_{hH^+H^-} = -i \frac{e}{m_W \sin \theta_W} (m_{H^\pm}^2 - \mu_2^2). \quad (8)$$

It is clear that from this equation the sign of the charged Higgs contribution to the triangular loop can be positive or negative, depending on the sizes of m_{H^+} and μ_2 . Thus, if we set

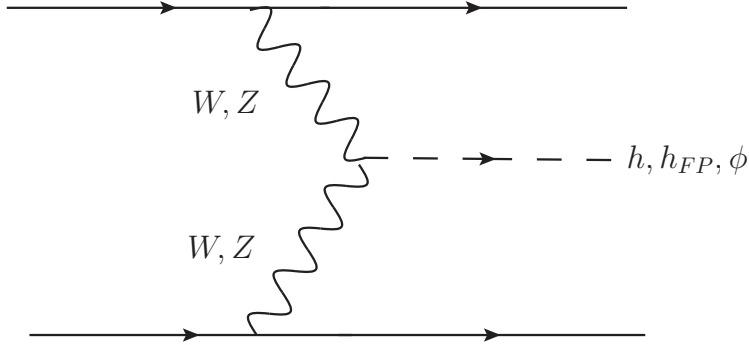


FIG. 1. A Feynman diagram showing the vector-boson fusion into SM Higgs, FP Higgs or radion.

$m_{H^\pm} = \mu_2$, the charged Higgs contribution vanishes and so the diphoton branching ratio becomes the same as the SM one.

It was shown in Ref. [33] that in gluon fusion the diphoton production rate is determined by the product of gluon-fusion cross section and the $\gamma\gamma$ branching ratio

$$\frac{\sigma(gg \rightarrow h) B(h \rightarrow \gamma\gamma)}{\sigma(gg \rightarrow h)_{\text{SM}} B(h \rightarrow \gamma\gamma)_{\text{SM}}} = \frac{B(h \rightarrow \gamma\gamma)}{B(h \rightarrow \gamma\gamma)_{\text{SM}}}, \quad (9)$$

which can be varied from about 0.5 to 2. The charged Higgs contribution to the diphoton branching ratio depends on the sizes of m_{H^\pm} and μ_2 . It was shown in Ref. [33] that when $m_{H^\pm}^2 < \mu_2^2$ the diphoton branching ratio is enhanced. Together with other theoretical constraints one can find the region to be $|\mu_2| \approx 100 - 200$ GeV and $m_{H^\pm} < |\mu_2|$.

III. VECTOR-BOSON FUSION (VBF)

The most distinguished feature of VBF at hadronic colliders is the appearance of two energetic forward jets separated by a large $\Delta R = \sqrt{(\Delta\eta)^2 + (\Delta\phi)^2}$, where η is the pseudo-rapidity and ϕ is the azimuth angle. The Feynman diagram is shown in Fig. 1. Each of the initial quarks radiates a W/Z boson, which further annihilates into the Higgs boson or some other particles under consideration. The unique feature of this process is that the W/Z bosons participating in the fusion process are close to on-shell [47], and irrespective whether the W/Z is longitudinal or transverse, the scattered quark carries almost all the energy of the incoming quark and goes in the forward direction.” [36, 37]. This fact justifies the use of effective W approximation in all calculations for VBF in the early days. Based on this feature we impose the following experimental cuts in selecting the dijet events coming

dominantly from the VBF:

$$E_{T_j} > 30 \text{ GeV}, \quad |\eta_j| < 4.7, \quad \Delta R_{jj} > 3.5, \quad (10)$$

and

$$\begin{aligned} (\text{Ejcut}) \quad E_{j_1} > 500 \text{ GeV} \quad \text{or} \\ (\text{Mjjcut}) \quad M_{jj} > 350 \text{ GeV}, \end{aligned} \quad (11)$$

where the subscript “1” denotes the most energetic jet. In the cut of Eq. (11), we choose either the energy of the most energetic jet $E_{j_1} > 500 \text{ GeV}$ or the invariant mass of the jet pair $M_{jj} > 350 \text{ GeV}$. This set of cuts is similar to that used by CMS [48] and ATLAS [49] in their searches for FP Higgs boson.

The vector-boson fusion is well-known that it allows to probe the direct coupling between the vector bosons and the Higgs boson or other particles under consideration. This is in contrast to the gg fusion, because any colored particles can flow in the triangular loop and affect the production rate. For example, in MSSM all squarks can circulate inside the loop.

IV. DECAY BRANCHING RATIOS

Here we list the decay branching ratio into $\gamma\gamma$ for the SM Higgs boson, fermiophobic Higgs boson, and the radion of mass 125 GeV in Table I. For the SM Higgs boson the decay into $\gamma\gamma$ goes through a triangle loop of W boson and top quark, between which they interfere destructively. The SM Higgs diphoton branching ratio is about 2.3×10^{-3} . This is very different for the FP Higgs boson, which allows only the W boson flowing in the loop. Thus, the branching ratio of a FP Higgs boson into diphoton can be an order of magnitude larger than that of the SM Higgs boson, and also because it does not decay into fermions. That is the reason why it can account for the observed 125 Higgs boson at the LHC, even though its gluon fusion production cross section is very small. The case of the radion is opposite to the FP Higgs. The diphoton branching ratio of the radion is a few times smaller than that of the SM, while its production rate via gg fusion is substantially enhanced.

We also list the branching ratio into $\gamma\gamma$ for the Higgs boson in the IHDM for a number of choices of parameters of the model in Table I, such that the diphoton branching ratio is enhanced relative to the SM one: $|\mu_2| \approx 100\text{--}200 \text{ GeV}$ and $m_{H^\pm} < |\mu_2|$. The factors affecting

TABLE I. Decay branching ratio $B(h \rightarrow \gamma\gamma)$ for the SM Higgs boson h_{SM} , the fermiophobic Higgs boson h_{FP} , the radion ϕ , the inert Higgs doublet model, the two Higgs doublet model, and the MSSM.

Parameter Space		$B(h \rightarrow \gamma\gamma)$			
SM		2.3×10^{-3}			
FP		1.5×10^{-2}			
Radion	$\Lambda_\phi = 0.8 - 1 \text{ TeV}$	0.57×10^{-3}			
$\mu_2 \text{ (GeV)} \quad m_{H^\pm} \text{ (GeV)}$					
IHDM1	200 70	6.7×10^{-3}			
IHDM2	200 100	3.3×10^{-3}			
IHDM3	200 150	2.5×10^{-3}			
IHDM4	200 200	2.3×10^{-3}			
IHDM5	150 70	4.2×10^{-3}			
IHDM10	100 90	2.4×10^{-3}			
$\sin \alpha \quad \tan \beta$					
2HDM1	0 1.5	3.8×10^{-3}			
2HDM2	0 5	6.5×10^{-3}			
2HDM3	0 10	6.8×10^{-3}			
2HDM4	0 20	6.9×10^{-3}			
MSSM					
	$m_{L_3} = m_{E_3}$	μ	m_h	$B(h \rightarrow \gamma\gamma)$	$\frac{\sigma(gg \rightarrow h)B(h \rightarrow \gamma\gamma)}{\sigma(gg \rightarrow h_{\text{SM}})B(h_{\text{SM}} \rightarrow \gamma\gamma)}$
BP1	250	400	127.0	2.4×10^{-3}	1.02
BP2	250	500	126.2	2.9×10^{-3}	1.19
BP3	250	536	125.4	3.6×10^{-3}	1.45
BP4	300	536	126.8	2.4×10^{-3}	1.005
BP5	300	700	125.4	2.8×10^{-3}	1.15
BP6	300	763	123.7	3.4×10^{-3}	1.38
BP7	350	700	126.6	2.4×10^{-3}	0.999
BP8	350	800	125.8	2.5×10^{-3}	1.03
BP9	350	927	123.9	2.7×10^{-3}	1.11

the partial width into $\gamma\gamma$ are the charged Higgs boson mass and the coupling $g_{hH^+H^-}$. The charged Higgs loop contribution can interfere either constructively or destructively with the SM contributions. Another factor that would affect the branching ratio into $\gamma\gamma$ is whether the thresholds into SS , AA , or H^+H^- are open. However, for our choices for m_S , m_{H^+} and m_A these decays would not be allowed. The diphoton branching ratio can be made similar to the SM one or enhanced by a few times.

The branching ratios into $\gamma\gamma$ for the light CP-even Higgs boson in the 2HDM for a number of choices of parameters of the model are shown in Table I, such that the enhancement in branching ratio can be achieved roughly along $\sin\alpha \approx 0$. Similar to IHDM, the main factors affecting the partial width into $\gamma\gamma$ are the charged Higgs boson mass and the coupling $g_{hH^+H^-}$. The branching ratio, on the other hand, also depends on other parameters such as $\tan\beta$ and $\sin\alpha$ as exhibited in the hWW and $ht\bar{t}$ couplings. Along $\sin\alpha \approx 0$, the factor $\cos\alpha \approx 1$ and the factor $\sin(\beta - \alpha) \approx 1$ for large $\tan\beta$, and thus the couplings hWW and $ht\bar{t}$ are close to their SM values. On the other hand, along $\sin\alpha = -1$ for large $\tan\beta$, the hWW coupling proportional to $\sin(\beta - \alpha)$ is only about $1/\tan\beta$. That is the reason why its branching ratio into $\gamma\gamma$ is very small.

In the MSSM, we choose the region where the lighter CP-even Higgs boson is around 125 GeV (123 – 128 GeV) and the diphoton production rate $\sigma(gg \rightarrow h)B(h \rightarrow \gamma\gamma)$ is equal to or larger than the SM value. As explained above the stop sector must be heavy in order to achieve a mass of 125 GeV for the lighter CP-even Higgs boson. First, we fix the $m_{Q_3} = m_{U_3} = 850$ GeV and $A_t = 1.4$ TeV with $\tan\beta = 60$ and $m_A = 1$ TeV. Second, we vary $m_{E_3} = m_{L_3}$ and μ to achieve a light stau so as to enhance the diphoton production rate, according to Eq. (4). We used the FeynHiggs [50] to evaluate the branching ratio $B(h \rightarrow \gamma\gamma)$ and the diphoton production rate $\sigma(gg \rightarrow h)B(h \rightarrow \gamma\gamma)$ relative to the SM values. We show in Fig. 2 the region in the plane of $(m_{E_3} = m_{L_3}, \mu)$ that the $m_h = 123 - 128$ GeV and the ratio $\sigma(gg \rightarrow h)B(h \rightarrow \gamma\gamma)/\sigma(gg \rightarrow h_{\text{SM}})B(h_{\text{SM}} \rightarrow \gamma\gamma)$ is larger than 1. We also show the branching ratios into $\gamma\gamma$ for the lighter CP-even Higgs boson and the inclusive diphoton production rate for a few selective points of MSSM in Table I.

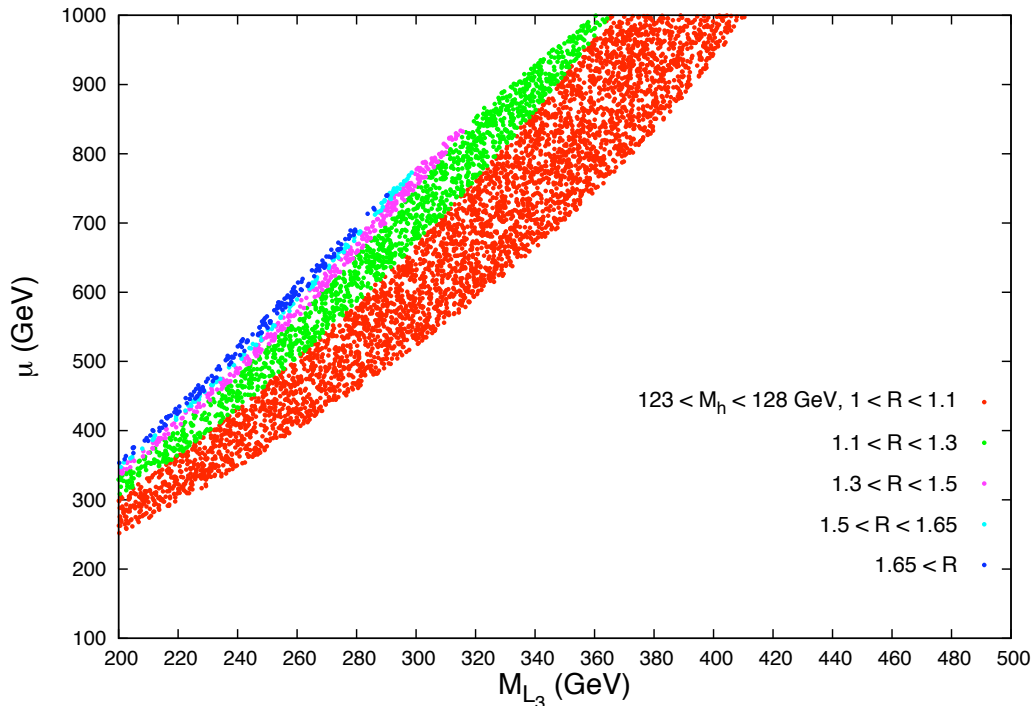


FIG. 2. The parameter space region where $m_h = 123 - 128$ GeV and $R = \sigma(gg \rightarrow h)B(h \rightarrow \gamma\gamma)/\sigma(gg \rightarrow h_{\text{SM}})B(h_{\text{SM}} \rightarrow \gamma\gamma)$ is larger than 1. The other fixed parameters are $m_{Q_3} = m_{U_3} = 850$ GeV, $A_t = 1.4$ TeV, $\tan\beta = 60$ and $m_A = 1$ TeV.

V. PRODUCTION RATES IN VECTOR-BOSON FUSION

We calculate the VBF cross sections for $pp \rightarrow jjh$ for various models under consideration. We impose the selection cuts for energetic forward jets as in Eqs. (10) and (11). We let the Higgs boson decay into $\gamma\gamma$, and impose the following cuts on the photons:

$$E_{T\gamma} > 30 \text{ GeV}, \quad |\eta_\gamma| < 2.5, \quad |m_{\gamma\gamma} - m_h| < 3.5 \text{ GeV}. \quad (12)$$

In the following, we present numerical results in both parton level and detector-simulation level by employing the PYTHIA-PGS (PYTHIA v6.420, PGS4(090401)) package inside MADGRAPH [51].

We employ MADGRAPH [51] to calculate the production cross sections for $pp \rightarrow jjh \rightarrow jj\gamma\gamma$ and implementing the selection cuts for the forward jets and the diphoton. The produc-

TABLE II. Production rates in fb at PGS level for $pp \rightarrow jjh \rightarrow jj\gamma\gamma$ at LHC-7 (LHC-8, LHC-14)

	photon cuts and E _{jcut}	photon cuts and M _{jcut}
SM	0.15 (0.19, 0.61)	0.33 (0.41, 1.1)
FP	1.03 (1.27, 4.12)	2.24 (2.78, 7.35)
Radion	0.0038 (0.0047, 0.014)	0.0076 (0.0095, 0.026)
IDHM1	0.44 (0.56, 1.79)	0.97 (1.21, 3.23)
IDHM2	0.22 (0.28, 0.88)	0.48 (0.59, 1.59)
IDHM3	0.16 (0.21, 0.67)	0.36 (0.45, 1.21)
IDHM4	0.15 (0.19, 0.62)	0.33 (0.41, 1.11)
IDHM5	0.28 (0.35, 1.12)	0.61 (0.76, 2.03)
IDHM10	0.16 (0.20, 0.64)	0.35 (0.43, 1.16)
2HDM1	0.17 (0.22, 0.70)	0.38 (0.47, 1.25)
2HDM2	0.41 (0.52, 1.66)	0.90 (1.11, 2.99)
2HDM3	0.44 (0.56, 1.79)	0.97 (1.20, 3.23)
2HDM4	0.45 (0.58, 1.85)	1.00 (1.24, 3.33)
MSSM BP	photon cuts and E _{jcut}	photon cuts and M _{jcut}
BP1	0.19 (0.28, 0.83)	0.44 (0.57, 1.47)
BP2	0.22 (0.33, 0.97)	0.52 (0.66, 1.76)
BP3	0.29 (0.40, 1.18)	0.63 (0.82, 2.10)
BP4	0.19 (0.28, 0.85)	0.43 (0.56, 1.46)
BP5	0.22 (0.32, 0.92)	0.50 (0.65, 1.65)
BP6	0.27 (0.38, 1.07)	0.61 (0.75, 1.90)
BP7	0.20 (0.26, 0.85)	0.43 (0.53, 1.47)
BP8	0.21 (0.29, 0.85)	0.44 (0.59, 1.48)
BP9	0.22 (0.30, 0.92)	0.49 (0.59, 1.66)

tion rates of diphoton for various models are then obtained by multiplying the corresponding diphoton branching ratios.

We use PYTHIA [52] for parton showering and hadronization. During the parton showering we turn on the initial and final state QED and QCD radiations (ISR and FSR), and fragmentation/hadronization according to the Lund model. We use PGS [53] for detector-

simulation with the most general settings for the LHC. Electromagnetic and hadronic calorimeter resolutions are set at $0.2/\sqrt{E}$ and $0.8/\sqrt{E}$, respectively. We use the cone algorithm for jet finding with a cone size of $\Delta R = 0.5$, Sagitta resolution of $13 \mu\text{m}$ ($\delta p_T/p_T = 1.04 \times 10^{-4}$), track-finding efficiency of 0.98, and minimum track p_T of 1 GeV. More details can be found in Refs. [51, 53].

The numerical results for LHC-7, LHC-8, and LHC-14 are listed in Table II for the SM, FP, radion, IHDM, 2HDM, and the MSSM.

It would be more transparent to show the production rate relative to the SM one

$$\frac{\sigma(pp \rightarrow jjX) \times B(X \rightarrow \gamma\gamma)}{\sigma(pp \rightarrow jjh_{\text{SM}}) \times B(h_{\text{SM}} \rightarrow \gamma\gamma)}, \quad (13)$$

where X stands for the SM Higgs or any other Higgs-like candidate in various models. We found that this ratio is quite robust against various cuts (M_{jcut} or E_{jcut} as in Eq. (11)) and against the energy of the collision.

In the upper panel of Fig. 3, we first show the ratio for the *inclusive* diphoton production rate $\frac{\sigma(X) \times B(X \rightarrow \gamma\gamma)}{\sigma(h_{\text{SM}}) \times B(h_{\text{SM}} \rightarrow \gamma\gamma)}$ of each model, which is dominated by gluon fusion, except for the FP Higgs boson. The parameter space of each model is chosen such that this inclusive diphoton rate is equal to or larger than the SM rate except for the FP Higgs boson which has no free parameter. For the same parameter space, we show in the lower panel the ratio for the *exclusive* $jj\gamma\gamma$ production rate $\frac{\sigma(pp \rightarrow jjX) \times B(X \rightarrow \gamma\gamma)}{\sigma(pp \rightarrow jjh_{\text{SM}}) \times B(h_{\text{SM}} \rightarrow \gamma\gamma)}$ for each model. The figure is valid for LHC-7, LHC-8 and LHC-14, and for using either M_{jcut} cut on both forward jets or E_{jcut} cut on the most energetic jet.

It is clear that the models can be employed to explain the excess in the inclusive diphoton rates in some parameter space region, but for the same region of parameter space the ratio of exclusive VBF production would be different among the models. The FP Higgs would be a number of times larger than the SM in the VBF channel, but the RS radion would give negligible exclusive VBF production. On the other hand, the IHDM, 2HDM, and the MSSM would give similar ratios in both inclusive and exclusive production. The 2HDM can give a somewhat smaller ratio in the exclusive VBF.

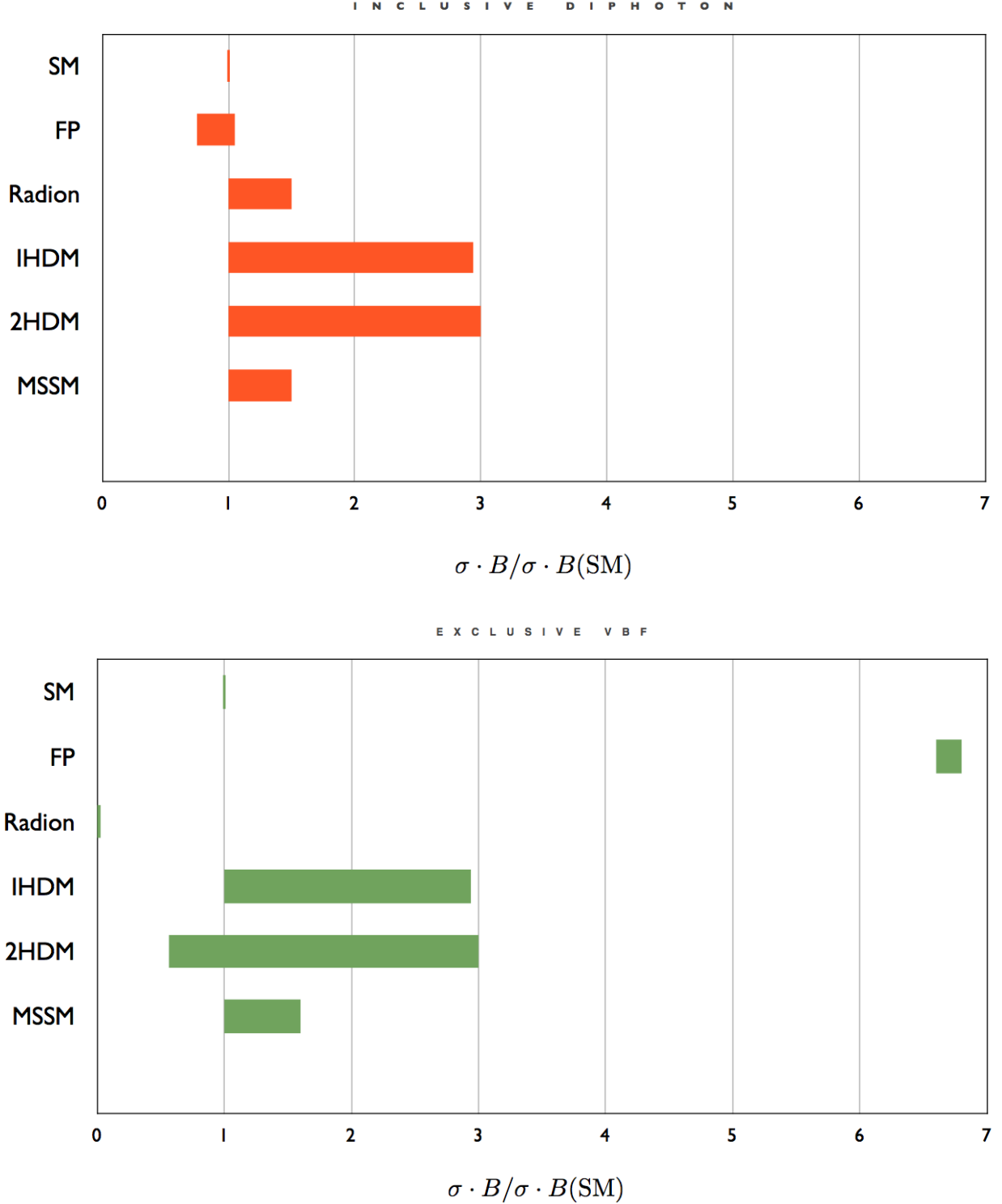


FIG. 3. *Upper:* the ratio of *inclusive* diphoton production rates $\frac{\sigma(X) \times B(X \rightarrow \gamma\gamma)}{\sigma(h_{\text{SM}}) \times B(h_{\text{SM}} \rightarrow \gamma\gamma)}$ for various models. The parameter space is chosen such that the ratio is equal to or larger than 1, except for the FP Higgs boson which has no free parameter. *Lower:* the ratio of the *exclusive* $jj\gamma\gamma$ production rate $\frac{\sigma(pp \rightarrow jjX) \times B(X \rightarrow \gamma\gamma)}{\sigma(pp \rightarrow jjh_{\text{SM}}) \times B(h_{\text{SM}} \rightarrow \gamma\gamma)}$ for each model in the corresponding parameter space.

A. Background Discussion

The experimental details for VBF in the context of searching for the FP Higgs boson are given in Ref. [48]. The dominant backgrounds to $h \rightarrow \gamma\gamma$ consist of i) the irreducible background from the prompt diphoton production, and ii) the reducible backgrounds from $pp \rightarrow \gamma + j$ and $pp \rightarrow jj$, when one or more of the jets hadronize into (typically neutral) pions and deposit energy in the electromagnetic calorimeter. These reconstructed objects are generally referred to as fake photons. Isolation is a very useful tool to reject the non-prompt background coming from electromagnetic showers originating in jets, because these fake photons are often accompanied by single and multiple π^0 s.

The dijet tag, as defined in Eqs. (10) and (11), together with the Higgs boson decaying into diphoton selects a special class of events consisting of two photons and two forward energetic jets. A signal-to-background ratio of order 1 can be achieved [48]. The signal from $h \rightarrow \gamma\gamma$ will be identified as a sharp peak in the $m_{\gamma\gamma}$ distribution, where the background is in continuum. In Ref. [48], the background model is derived from data. In the new run at 8 TeV, we expect the same treatment is applied to the background. The estimation of significance of each signal is beyond the scope of the present paper.

Given that we have obtained the event rates of each model in the tables, which have been under experimental cuts and simulations (PGS), it is straight-forward to estimate the required luminosity to probe various scenarios. The continuum background at the 7 TeV and 8 TeV LHC in VBF channel has been obtained in Refs. [48] and [2]. Since the SM Higgs boson has been seen above the background with some significance level in the VBF channel in the current LHC runs (about 5 fb^{-1} at 7 TeV and **about** 5 fb^{-1} at 8 TeV), the scenarios with higher event rates than the SM Higgs boson should be detectable. The projected integrated luminosity at the end of 2012 is about $10 - 15 \text{ fb}^{-1}$ for each experiment, it would not be a problem to investigate the scenarios in the VBF channel.

VI. CONCLUSIONS

LHC is expected to confirm if there is a new particle at 125 GeV by the end of this year. The likelihood for a new discovery is rather high. Nevertheless, whether this new particle is the SM Higgs boson is not an easy question to answer.

Here the scenario of this 125 GeV particle produced by vector-boson fusion, instead of gluon fusion as the dominant production mechanism for the standard model Higgs boson, is studied in details. By using the forward dijet tagging technique, one can single out the vector-boson fusion mechanism. We studied a number of popular new physics models that have been employed to interpret the observed particle at 125 GeV, including fermiophobic Higgs boson, the Randall-Sundrum radion, inert-Higgs-doublet model, two-Higgs-doublet model, and the MSSM. Since the inclusive diphoton channel showed an excess over the SM predictions, we first selected the parameter space of each model that can give an inclusive diphoton rate larger than or equal to the SM rate. Then, we calculate the exclusive $jj\gamma\gamma$ diphoton production rate in VBF for that parameter space. If the diphoton mode excess seen at LHC-7 can be firmly established by the new LHC-8 data, it will be the utmost task to identify the nature of this particle. Perhaps, it is simply the SM Higgs boson with some level of statistical fluctuation, but it could also be the RS radion [32], fermiophobic Higgs boson [31], the light CP-even Higgs boson of the 2HDM [30], the Higgs boson of the IHDM [33], or one of the CP-even Higgs bosons in other extensions of the MSSM [27, 28], all of which can allow an enhancement to the $\gamma\gamma$ production rate. On the other hand, the vector-boson fusion, as singled out by the dijet tag, provides useful information in helping to differentiate among various models. It is not hard by browsing through Fig. 3 to conclude the following

- If a similar rate is seen in inclusive production but no large excess is seen in the exclusive VBF production it would unlikely be a fermiophobic Higgs boson.
- If a similar rate or excess is seen in inclusive production but some events are seen in exclusive VBF production rate, it would unlikely be the RS radion.
- If moderate excess is seen in both inclusive production and exclusive VBF production, it could be the Higgs boson of the IHDM, 2HDM, or the MSSM. However, if the excess is over 60% it will pose severe challenge to the MSSM.

It seems easy to rule out either fermiophobic Higgs boson or RS radion, providing that we see no large excess or some events in VBF channel, respectively. However, it is still difficult to distinguish the other models when the inclusive and exclusive rates are similar to or slightly larger than the SM values. If the production rate of the diphoton mode at 125 GeV lines up

with the SM prediction eventually, it is still premature to conclude this is coming from the SM Higgs boson. Other alternatives in MSSM, NMSSM, or other SUSY models can also be mimicking the SM Higgs boson, depending on the parameter space of the new physics model. In any case, once the signals at 125 GeV are confirmed further studies including all possible decay modes are to be taken into account in order to discriminate these many alternatives beyond the standard model.

Vector-boson fusion is the next most important production mechanism that must be taken into account to fully identify the newly discovered particle.

ACKNOWLEDGMENT

This work was supported in part by the National Science Council of Taiwan under Grants No. 99-2112-M-007-005-MY3 and No. 101-2112-M-001-005-MY3 as well as the WCU program through the KOSEF funded by the MEST (R31-2008-000-10057-0).

-
- [1] G. Aad *et al.* [The ATLAS Collaboration], arXiv:1207.7214 [hep-ex].
 - [2] S. Chatrchyan *et al.* [The CMS Collaboration], arXiv:1207.7235 [hep-ex].
 - [3] P. W. Higgs, Phys. Rev. Lett. **13**, 508 (1964); F. Englert and R. Brout, Phys. Rev. Lett. **13**, 321 (1964); G. S. Guralnik, C. R. Hagen and T. W. B. Kibble, Phys. Rev. Lett. **13**, 585 (1964).
 - [4] E. Farhi and L. Susskind, Phys. Rept. **74**, 277 (1981).
 - [5] H. E. Haber and G. L. Kane, Phys. Rept. **117**, 75 (1985).
 - [6] N. Arkani-Hamed, S. Dimopoulos and G. R. Dvali, Phys. Rev. D **59**, 086004 (1999) [hep-ph/9807344].
 - [7] T. Appelquist, H. -C. Cheng and B. A. Dobrescu, Phys. Rev. D **64**, 035002 (2001) [hep-ph/0012100].
 - [8] L. Randall and R. Sundrum, Phys. Rev. Lett. **83**, 3370 (1999) [hep-ph/9905221].
 - [9] N. Arkani-Hamed, A. G. Cohen, E. Katz and A. E. Nelson, JHEP **0207**, 034 (2002) [hep-ph/0206021].

- [10] R. Bernabei *et al.* [DAMA and LIBRA Collaborations], *Eur. Phys. J. C* **67**, 39 (2010) [arXiv:1002.1028 [astro-ph.GA]].
- [11] C. E. Aalseth *et al.* [CoGeNT Collaboration], *Phys. Rev. Lett.* **106**, 131301 (2011) [arXiv:1002.4703 [astro-ph.CO]].
- [12] Z. Ahmed *et al.* [CDMS-II Collaboration], *Science* **327**, 1619 (2010) [arXiv:0912.3592 [astro-ph.CO]].
- [13] E. Aprile *et al.* [XENON100 Collaboration], arXiv:1207.5988 [astro-ph.CO].
- [14] D. Tucker-Smith and N. Weiner, *Phys. Rev. D* **64**, 043502 (2001) [hep-ph/0101138].
- [15] J. L. Feng, J. Kumar, D. Marfatia and D. Sanford, *Phys. Lett. B* **703**, 124 (2011) [arXiv:1102.4331 [hep-ph]].
- [16] K. M. Zurek, *Phys. Rev. D* **79**, 115002 (2009) [arXiv:0811.4429 [hep-ph]].
- [17] T. Aaltonen *et al.* [CDF Collaboration], *Phys. Rev. Lett.* **101**, 202001 (2008) [arXiv:0806.2472 [hep-ex]]; T. Aaltonen *et al.* [CDF Collaboration], *Phys. Rev. D* **83**, 112003 (2011) [arXiv:1101.0034 [hep-ex]]; V. M. Abazov *et al.* [D0 Collaboration], *Phys. Rev. D* **84**, 112005 (2011) [arXiv:1107.4995 [hep-ex]].
- [18] S. Jung, H. Murayama, A. Pierce and J. D. Wells, *Phys. Rev. D* **81**, 015004 (2010) [arXiv:0907.4112 [hep-ph]]; K. Cheung, W. -Y. Keung and T. -C. Yuan, *Phys. Lett. B* **682**, 287 (2009) [arXiv:0908.2589 [hep-ph]]; J. Shu, T. M. P. Tait and K. Wang, *Phys. Rev. D* **81**, 034012 (2010) [arXiv:0911.3237 [hep-ph]]; P. H. Frampton, J. Shu and K. Wang, *Phys. Lett. B* **683**, 294 (2010) [arXiv:0911.2955 [hep-ph]].
- [19] S. Chatrchyan *et al.* [CMS Collaboration], *Phys. Lett. B* **709**, 28 (2012) [arXiv:1112.5100 [hep-ex]]; J. A. Aguilar-Saavedra and M. Perez-Victoria, *JHEP* **1109**, 097 (2011) [arXiv:1107.0841 [hep-ph]].
- [20] T. Aaltonen *et al.* [CDF Collaboration], *Phys. Rev. Lett.* **106**, 171801 (2011) [arXiv:1104.0699 [hep-ex]].
- [21] K. Cheung and J. Song, *Phys. Rev. Lett.* **106**, 211803 (2011) [arXiv:1104.1375 [hep-ph]]; A. E. Nelson, T. Okui and T. S. Roy, *Phys. Rev. D* **84**, 094007 (2011) [arXiv:1104.2030 [hep-ph]]. X. -P. Wang, Y. -K. Wang, B. Xiao, J. Xu and S. -h. Zhu, *Phys. Rev. D* **83**, 115010 (2011) [arXiv:1104.1917 [hep-ph]]. F. Yu, *Phys. Rev. D* **83**, 094028 (2011) [arXiv:1104.0243 [hep-ph]]; M. R. Buckley, D. Hooper, J. Kopp and E. Neil, *Phys. Rev. D* **83**, 115013 (2011) [arXiv:1103.6035 [hep-ph]]. P. J. Fox, J. Liu, D. Tucker-Smith and N. Weiner, *Phys. Rev. D*

- 84**, 115006 (2011) [arXiv:1104.4127 [hep-ph]]; E. J. Eichten, K. Lane and A. Martin, Phys. Rev. Lett. **106**, 251803 (2011) [arXiv:1104.0976 [hep-ph]].
- [22] V. M. Abazov *et al.* [D0 Collaboration], Phys. Rev. Lett. **107**, 011804 (2011) [arXiv:1106.1921 [hep-ex]]; S. Chatrchyan *et al.* [CMS Collaboration], arXiv:1208.3477 [hep-ex].
- [23] G. Aad *et al.* [ATLAS Collaboration], Phys. Lett. B **710**, 49 (2012) [arXiv:1202.1408 [hep-ex]]; S. Chatrchyan *et al.* [CMS Collaboration], Phys. Lett. B **710**, 26 (2012) [arXiv:1202.1488 [hep-ex]].
- [24] J. Chang, K. Cheung, P. -Y. Tseng and T. -C. Yuan, arXiv:1206.5853 [hep-ph].
- [25] M. Carena, S. Gori, N. R. Shah and C. E. M. Wagner, JHEP **1203**, 014 (2012) [arXiv:1112.3336 [hep-ph]]; M. Carena, S. Gori, N. R. Shah, C. E. M. Wagner and L. -T. Wang, JHEP **1207**, 175 (2012) [arXiv:1205.5842 [hep-ph]].
- [26] H. Baer, V. Barger and A. Mustafayev, Phys. Rev. D **85**, 075010 (2012) [arXiv:1112.3017 [hep-ph]]; S. Heinemeyer, O. Stal and G. Weiglein, Phys. Lett. B **710**, 201 (2012) [arXiv:1112.3026 [hep-ph]]; A. Arbey, M. Battaglia, A. Djouadi, F. Mahmoudi and J. Quevillon, Phys. Lett. B **708**, 162 (2012) [arXiv:1112.3028 [hep-ph]]; P. Draper, P. Meade, M. Reece and D. Shih, Phys. Rev. D **85**, 095007 (2012) [arXiv:1112.3068 [hep-ph]]; S. Akula, B. Altunkaynak, D. Feldman, P. Nath and G. Peim, Phys. Rev. D **85**, 075001 (2012) [arXiv:1112.3645 [hep-ph]]; M. Kadastik, K. Kannike, A. Racioppi and M. Raidal, JHEP **1205**, 061 (2012) [arXiv:1112.3647 [hep-ph]]; J. Cao, Z. Heng, D. Li and J. M. Yang, Phys. Lett. B **710**, 665 (2012) [arXiv:1112.4391 [hep-ph]]; N. D. Christensen, T. Han and S. Su, arXiv:1203.3207 [hep-ph]; J. L. Feng and D. Sanford, Phys. Rev. D **86**, 055015 (2012) [arXiv:1205.2372 [hep-ph]]; J. -J. Cao, Z. -X. Heng, J. M. Yang, Y. -M. Zhang and J. -Y. Zhu, JHEP **1203**, 086 (2012) [arXiv:1202.5821 [hep-ph]]; T. Li, J. A. Maxin, D. V. Nanopoulos and J. W. Walker, Phys. Lett. B **710**, 207 (2012) [arXiv:1112.3024 [hep-ph]]; V. Barger, M. Ishida and W. -Y. Keung, arXiv:1207.0779 [hep-ph].
- [27] U. Ellwanger, JHEP **1203**, 044 (2012) [arXiv:1112.3548 [hep-ph]]; J. F. Gunion, Y. Jiang and S. Kraml, Phys. Lett. B **710**, 454 (2012) [arXiv:1201.0982 [hep-ph]]; S. F. King, M. Muhlleitner and R. Nevzorov, Nucl. Phys. B **860**, 207 (2012) [arXiv:1201.2671 [hep-ph]]; J. Cao, Z. Heng, J. M. Yang, Y. Zhang and J. Zhu, JHEP **1203**, 086 (2012) [arXiv:1202.5821 [hep-ph]]; U. Ellwanger and C. Hugonie, arXiv:1203.5048 [hep-ph]; D. A. Vasquez, G. Belanger, C. Boehm, J. Da Silva, P. Richardson and C. Wymant, Phys. Rev. D **86**, 035023 (2012) [arXiv:1203.3446

- [hep-ph]].
- [28] C. -F. Chang, K. Cheung, Y. -C. Lin and T. -C. Yuan, JHEP **1206** 128 (2012), [arXiv:1202.0054 [hep-ph]].
- [29] M. Hirsch, W. Porod, L. Reichert and F. Staub, arXiv:1206.3516 [hep-ph]; H. An, T. Liu and L. -T. Wang, arXiv:1207.2473 [hep-ph]; P. Athron, S. F. King, D. J. Miller, S. Moretti and R. Nevzorov, arXiv:1206.5028 [hep-ph]; K. S. Jeong, Y. Shoji and M. Yamaguchi, JHEP **1209**, 007 (2012) [arXiv:1205.2486 [hep-ph]]; F. Boudjema and G. D. La Rochelle, Phys. Rev. D **86**, 015018 (2012) [arXiv:1203.3141 [hep-ph]]; P. Fileviez Perez, Phys. Lett. B **711**, 353 (2012) [arXiv:1201.1501 [hep-ph]].
- [30] P. M. Ferreira, R. Santos, M. Sher and J. P. Silva, Phys. Rev. D **85**, 077703 (2012) [arXiv:1112.3277 [hep-ph]]; G. Burdman, C. E. F. Haluch and R. D. Matheus, Phys. Rev. D **85**, 095016 (2012) [arXiv:1112.3961 [hep-ph]]; E. Cervero and J. -M. Gerard, Phys. Lett. B **712**, 255 (2012) [arXiv:1202.1973 [hep-ph]]; P. M. Ferreira, R. Santos, M. Sher and J. P. Silva, Phys. Rev. D **85**, 035020 (2012) [arXiv:1201.0019 [hep-ph]]; N. Chen and H. -J. He, JHEP **1204**, 062 (2012) [arXiv:1202.3072 [hep-ph]]; A. Arhrib, R. Benbrik and C. -H. Chen, arXiv:1205.5536 [hep-ph]; H. S. Cheon and S. K. Kang, arXiv:1207.1083 [hep-ph]; W. Altmannshofer, S. Gori and G. D. Kribs, arXiv:1210.2465 [hep-ph]; N. Craig and S. Thomas, arXiv:1207.4835 [hep-ph]; D. S. M. Alves, P. J. Fox and N. J. Weiner, arXiv:1207.5499 [hep-ph]; S. Chang, S. K. Kang, J. -P. Lee, K. Y. Lee, S. C. Park and J. Song, arXiv:1210.3439 [hep-ph]; Y. Bai, V. Barger, L. L. Everett and G. Shaughnessy, arXiv:1210.4922 [hep-ph].
- [31] E. Gabrielli, B. Mele and M. Raidal, arXiv:1202.1796 [hep-ph]; E. L. Berger, Z. Sullivan and H. Zhang, arXiv:1203.6645 [hep-ph]; E. Gabrielli, K. Kannike, B. Mele, A. Racioppi and M. Raidal, Phys. Rev. D **86**, 055014 (2012) [arXiv:1204.0080 [hep-ph]].
- [32] K. Cheung and T. -C. Yuan, Phys. Rev. Lett. **108**, 141602 (2012) [arXiv:1112.4146 [hep-ph]]; V. Barger, M. Ishida and W. -Y. Keung, Phys. Rev. Lett. **108**, 101802 (2012) [arXiv:1111.4473 [hep-ph]]; *ibid.* Phys. Rev. D **85**, 015024 (2012) [arXiv:1111.2580 [hep-ph]]; B. Grzadkowski, J. F. Gunion and M. Toharia, Phys. Lett. B **712**, 70 (2012) [arXiv:1202.5017 [hep-ph]]; Y. Tang, arXiv:1204.6145 [hep-ph]; S. Matsuzaki and K. Yamawaki, Phys. Rev. D **85**, 095020 (2012) [arXiv:1201.4722 [hep-ph]]; H. de Sandes and R. Rosenfeld, Phys. Rev. D **85**, 053003 (2012) [arXiv:1111.2006 [hep-ph]].

- [33] A. Arhrib, R. Benbrik and N. Gaur, Phys. Rev. D **85**, 095021 (2012) [arXiv:1201.2644 [hep-ph]]; L. Wang and X. -F. Han, JHEP **1205**, 088 (2012) [arXiv:1203.4477 [hep-ph]].
- [34] P. Draper and D. McKeen, Phys. Rev. D **85**, 115023 (2012) [arXiv:1204.1061 [hep-ph]].
- [35] D. Carmi, A. Falkowski, E. Kuflik and T. Volansky, arXiv:1202.3144 [hep-ph]; A. Azatov, R. Contino and J. Galloway, JHEP **1204**, 127 (2012) [arXiv:1202.3415 [hep-ph]]; J. R. Espinosa, C. Grojean, M. Muhlleitner and M. Trott, JHEP **1205**, 097 (2012) [arXiv:1202.3697 [hep-ph]]; V. Barger, M. Ishida and W. -Y. Keung, Phys. Rev. Lett. **108**, 261801 (2012) [arXiv:1203.3456 [hep-ph]]; P. P. Giardino, K. Kannike, M. Raidal and A. Strumia, JHEP **1206**, 117 (2012) [arXiv:1203.4254 [hep-ph]]; J. Ellis and T. You, JHEP **1206**, 140 (2012) [arXiv:1204.0464 [hep-ph]]; A. Azatov, R. Contino, D. Del Re, J. Galloway, M. Grassi and S. Rahatlou, JHEP **1206**, 134 (2012) [arXiv:1204.4817 [hep-ph]]; M. Klute, R. Lafaye, T. Plehn, M. Rauch and D. Zerwas, arXiv:1205.2699 [hep-ph].
- [36] J. Bagger, V. D. Barger, K. -m. Cheung, J. F. Gunion, T. Han, G. A. Ladinsky, R. Rosenfeld and C. -P. Yuan, Phys. Rev. D **52**, 3878 (1995) [hep-ph/9504426].
- [37] D. L. Rainwater and D. Zeppenfeld, JHEP **9712**, 005 (1997) [hep-ph/9712271].
- [38] K. Cheung and O. C. W. Kong, Phys. Rev. D **68**, 053003 (2003) [hep-ph/0302111].
- [39] S. Akula, P. Nath and G. Peim, arXiv:1207.1839 [hep-ph]; P. Nath, arXiv:1210.0520 [hep-ph].
- [40] J. F. Gunion, H. E. Haber, G. L. Kane and S. Dawson, Front. Phys. **80**, 1 (2000).
- [41] K. Hagiwara, J. S. Lee and J. Nakamura, arXiv:1207.0802 [hep-ph].
- [42] A. G. Akeroyd, J. Phys. G **24**, 1983 (1998) [hep-ph/9803324].
- [43] W. Goldberger and M. Wise, Phys. Rev. Lett. **83**, 4922 (1999).
- [44] W. Goldberger and M. Wise, Phys. Lett. **B475** 275 (2000).
- [45] C. Csáki, M. Graesser, L. Randall and J. Terning, Phys. Rev. D **62**, 045015 (2000); C. Csáki, M. L. Graesser and G. D. Kribs, Phys. Rev. D **63**, 065002 (2001) [hep-th/0008151].
- [46] K. -m. Cheung, Phys. Rev. D **63**, 056007 (2001) [hep-ph/0009232]; W. D. Goldberger, B. Grinstein and W. Skiba, Phys. Rev. Lett. **100**, 111802 (2008) [arXiv:0708.1463 [hep-ph]].
- [47] M. S. Chanowitz, Ann. Rev. Nucl. Part. Sci. **38**, 323 (1988).
- [48] CMS Collaboration, “Search for the fermiophobic model Higgs boson decaying into two photons”, CMS-PAS-HIG-12-002, March 2012.
- [49] ATLAS Collaboration, “Search for a fermiophobic Higgs boson in the diphoton decay channel with 4.9 fb¹ of ATLAS data at $\sqrt{s} = 7$ TeV”, ATLAS-CONF-2012-13, March 2012.

- [50] M. Frank, T. Hahn, S. Heinemeyer, W. Hollik, H. Rzehak and G. Weiglein, JHEP **0702**, 047 (2007) [hep-ph/0611326].
- [51] MADGRAPH: J. Alwall, M. Herquet, F. Maltoni, O. Mattelaer and T. Stelzer, JHEP **1106**, 128 (2011) [arXiv:1106.0522 [hep-ph]].
- [52] T. Sjostrand, S. Mrenna and P. Z. Skands, Comput. Phys. Commun. **178**, 852 (2008) [arXiv:0710.3820 [hep-ph]].
- [53] The MG/ME Pythia-PGS package <http://madgraph.hep.uiuc.edu/index.html>, J. Alwall and the CP3 development team.